2022 IEEE International Conference on Robotics and Automation (ICRA)
May 23-27, 2022. Philadelphia, PA, USA

Systematic Development of a Novel, Dynamic, Reduced Complexity Quadruped Robot Platform for Robotic Tail Research

Yujiong Liu[1] and Pinhas Ben-Tzvi[1*]

Abstract— This paper presents a systematical approach to develop a novel reduced complexity quadruped (RCQ) robot designed for serpentine robotic tail research purposes. The critical design requirements are determined based on careful dynamic analysis and synthesis results. Guided by formulated design requirements and principles, a robot prototype was designed and built. The robot has an overall weight of 5 Kg and the body size of a domestic cat. The existing electronic system allows a control frequency of up to 1 kHz and accepts both torque and position commands. These features guarantee that the platform could be used to explore the dynamic usages of robotic tails on legged locomotion. The preliminary tests show that the hardware can lift itself off the ground up to 112 mm (46.7% of its body height) and stay in the air for at least 0.3 seconds.

I. INTRODUCTION

To improve the agility and controllability of moving robots, inspired by animals, researchers started mounting a robotic tail on mobile platforms [1]–[18]. Although impressive progress has been made over the past decade, this research is somehow still in its early stages and there are still many open problems to be solved. One of these problems is how (if possible) a serpentine robotic tail system [19] could help the dynamic locomotion of legged robots since we see that in nature, with the help of the tail, animals exhibit highly agile, aperiodic, and dexterous motions, such as cheetah's complicated behaviors during hunting [20] and kangaroo rat's superior escaping maneuver [21].

To explore this problem, a quadruped platform (as a starting point, a biped is not suitable due to its more challenging balance control) that is capable of dynamic locomotion is necessary. However, most existing quadruped robot platforms (e.g., the Big Dog [22], HyQ [23], ANYmal series [24], MIT Cheetah series [25], etc.) did not consider putting a tail on-board when they were developed, which left them with a limited modification space to integrate a robotic tail system, let alone a heavier (which has more actuators) serpentine robotic tail. Therefore, we proposed to use a reduced complexity quadruped (RCQ) as the first step to explore the dynamic usages of serpentine robotic tails on legged locomotion. The "reduced complexity" here refers to fewer degrees of freedom (DOF) in each leg and thus less weight, simpler control, and better dynamic capability. More importantly, this simplification does not sacrifice any of the important dynamic locomotion features of legged robots, e.g., under-actuation, ground contact, and path constraints, which are vital components of the original problem setting.

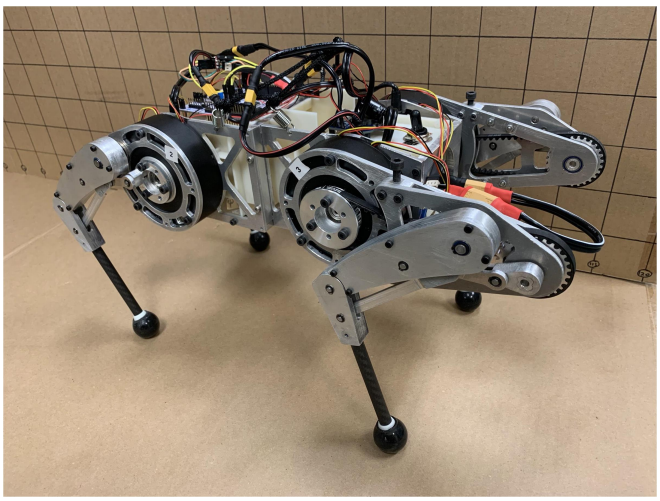

Fig. 1: Prototype of the reduced complexity quadruped (RCQ) robot with single DOF legs

Besides all these benefits, a potential but unique advantage (which needs to be verified) of the RCQ for the serpentine robotic tail is that from a control's perspective, these two systems may be complementary to each other. That is, the lost controllability from the legs is brought back by the increased controllability in the tail, although these two controllabilities may not be the same. If this advantage was proven to be true, it may bring about a new locomotion paradigm for legged robots, such that the legs are only responsible for propulsion while the tail(s) are responsible for maneuvering and stabilization. It is worth noting that this special locomotion paradigm was not purely artificial. In fact, many animals have already adopted this locomotion strategy, such as the mudskipper [26].

The main tradeoff of the RCQ idea is that the locomotion modes (including both periodic and aperiodic motions) are limited by the fixed foot trajectory. For the same reason, the design process requires more careful analysis and manufacturing. As long as the robot was assembled, there would be no room to adjust the foot trajectory. However, as the first step to explore the serpentine robotic tail usages on legged locomotion, these

[1]Yujiong Liu and Pinhas Ben-Tzvi are with the Robotics and Mechatronics Lab in the Mechanical Engineering Department, Virginia Tech, Blacksburg, VA 24060, USA {yjliu, bentzvi}@vt.edu

This work was supported by the National Science Foundation under Grant No. 1906727

*Corresponding author

2022 IEEE International Conference on Robotics and Automation (ICRA) | 978-1-7281-9681-7/22/$31.00 ©2022 IEEE | DOI: 10.1109/ICRA46639.2022.9811871

disadvantages are thought as acceptable.

Therefore, this paper aims to develop such a reduced complexity quadruped robot platform that is capable of fitting a serpentine robotic tail and is able to perform dynamic motions, e.g., using the tail to help the maneuvering and stabilization functions of the quadrupedal locomotion. The main contributions of this work are summarized as follows. First, a novel RCQ robot is proposed to help the robotic tail research. Second, a systematic design paradigm based on dynamic analysis and synthesis is proposed to determine the critical design constraints of the RCQ. Third, based on the formulated design requirements and principles, the detailed design of this new robot was carried out and a prototype was built (as shown in Fig. 1).

The rest of this paper is organized as follows. Section II systematically determines the design requirements and design principles based on dynamic analysis. Section III realizes the actual design based on the design constraints formulated in Section II. Section IV validates the design by prototyping and experiments. The conclusion section recaps the main points of this paper and discusses the future work.

II. DESIGN ANALYSIS AND SYNTHESIS

Although the quadruped robot is developed independently from the tail system, these two systems are intrinsically coupled and have to be considered as a whole. Therefore, dynamic analysis for the complete system must be conducted first, to determine the critical design requirements for the quadruped system. Fig. 2 shows the workflow of the design paradigm applied here, which mainly consists of two design iteration loops: one dynamic analysis loop to determine the critical dynamic parameters (e.g., tail-torso mass ratio, tail-torso length ratio, and the system center of mass (COM) location) through simulation, and one design iteration to make the actual design choices. This section mainly focuses on the dynamic analysis loop.

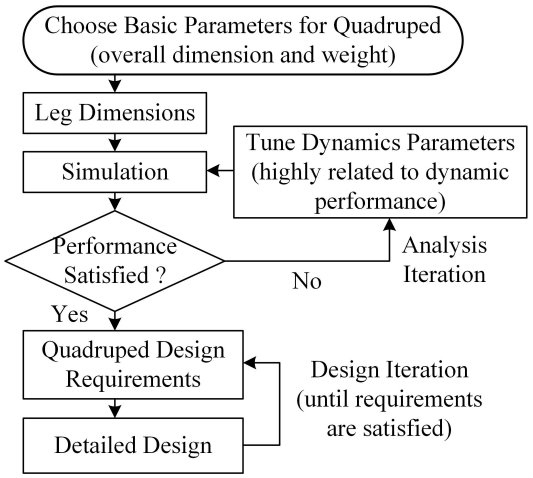

Fig. 2: Flowchart of the RCQ design paradigm

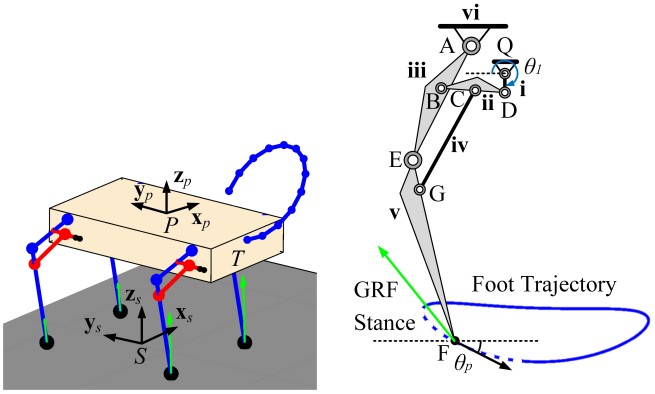

(a) (b)

Fig. 3: (a) The simulated quadruped model with a serpentine tail; (b) kinematic diagram of the leg mechanism together with its foot trajectory, where the dashed portion is for the stance phase. The green arrows are the ground reaction force (GRF) vectors.

The basic dimensions are chosen as 300 mm long, 200 mm wide, and 220 mm tall, all measured based on the hip joint positions. The initial masses are set as 6 Kg for the quadruped and 1.5 Kg for the tail system (including both the tail body and its actuation unit). For comparison purposes, the roll-revolute-revolute robotic tail (R3RT) [27] (3 DOFs, two independent segments) was selected as the benchmark tail system and a 20 degrees yaw maneuver is chosen as the standard motion. The model configuration is shown in Fig. 3a.

A. Kinematics and Dynamics

The single DOF leg mechanism is shown in Fig. 3b, which is essentially a Jansen mechanism [28] and its dimensions were optimized to execute a foot trajectory for trotting [29]. Its kinematics is defined by two vector loop equations:

$$\overrightarrow{QD}+\overrightarrow{DB}=\overrightarrow{QA}+\overrightarrow{AB} \tag{1}$$

$$\overrightarrow{CG}+\overrightarrow{GE}=\overrightarrow{CB}+\overrightarrow{BE} \tag{2}$$

where points B, C, D, and points E, G, F are collinear, respectively. Solving these two equations together with (3) yields the foot position $\boldsymbol{p}_f$ and differentiating (3) directly gives the Jacobian $\boldsymbol{J}_f$ of the foot position.

$$\overrightarrow{AF}=\overrightarrow{AE}+\overrightarrow{EF} \tag{3}$$

The system dynamics of the tailed robot is formulated as a floating base model assuming that the legs are massless (to simplify the dynamic model). Although the leg inertia is neglected, its motion can still induce the ground reaction forces (GRF), which in turn drive the locomotion of the robot. The GRF is calculated using a soft contact model [30]. With the dynamic model, extensive simulations using the ode45 function in MATLAB were performed to determine the satisfied

motion results. The detailed dynamic model, as well as the simulation settings, were previously published in [31], and readers are referred to this reference for more details. Here we take advantage of the existing simulation results to formulate the requirements for the actual design.

B. Actuator Sizing

Since the leg is assumed to be massless, the actuation torque of the crank (part i in Fig. 3b) does not appear in the dynamic model. However, this quantity could be estimated from the GRF through the Jacobians of the foot position:

$$\tau_c = j_{f,n} f_{f,n} + j_{f,h} f_{f,h} \tag{4}$$

where τ_c is the torque reflected on the crank, $j_{f,n}$ and $j_{f,h}$ are the normal and horizontal components (plotted in Fig. 4) of the foot Jacobian $\boldsymbol{J}_f$, respectively. Accordingly, $f_{f,n}$ and $f_{f,h}$ are the normal force and horizontal force (ground friction) components of the GRF, respectively. Note that (4) assumes an ideal transmission (no internal friction) for the leg mechanism. The required torque and power on the crank for the selected maneuvering motion are calculated and shown in Fig. 5, where the crank speed was a constant speed of -40 rad/s.

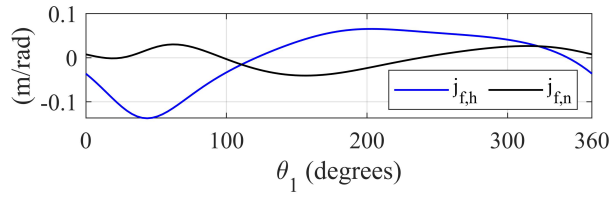

Fig. 4: Plots of the normal and horizontal Jacobian components for the leg mechanism

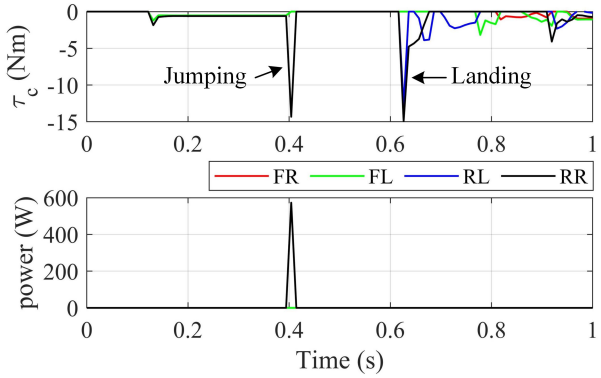

Fig. 5: Torque and power consumption required for the actuator

Therefore, the RCQ actuator requires a maximum capacity greater than 600 W and a maximum torque greater than 15 Nm. Since the actuator has both the power and torque requirements, the actuator needs to be selected to satisfy the motor capacity first and then to meet the torque requirement by choosing a proper gearbox reduction ratio.

C. Mass Distribution

Based on the results of [31], the system mass distribution is critical for the performance of the tailed quadruped, which mainly includes three parameters: the tail-torso mass ratio, the tail-torso length ratio, and the torso COM location (measured along $\mathbf{y}_p$ direction from the rear hip axes, with reference to Fig. 3a). The first two parameters are determined by the tail system and therefore, for the quadruped design purpose, only the third parameter, which was determined to be a value from 180 mm to 330 mm, is meaningful. However, this value is based on the assumption that all the mass of the tail actuation module (1 Kg) is concentrated at the tail mounting point T. In reality, this is neither practical nor necessary. The tail actuators could be deployed along the torso so that the tail system could be self-balanced. Considering this practical factor, the COM of the tail actuation module is moved to the torso geometric center P (the distance from P to T is 190 mm). This in turn requires a move of $190/6 \approx 32$ mm for the torso COM location along the $-\mathbf{y}_p$ direction, which gives the new torso COM location range from 148 mm to 298 mm.

D. Design Requirements and Principles

Based on the design analysis results, the robot design should satisfy the following requirements: (1) the hip joint positions should be exactly the same as the simulation setting; (2) the robot should weigh less than 6 Kg; (3) from the simulations, the quadruped is required to jump at least 100 mm high with a tail system. For the quadruped system alone, this jumping height requirement is raised to $100 \times 7.5/6 = 125$ mm; (4) the leg actuator should have a maximum capacity greater than 600 W and a maximum torque greater than 15 Nm; and (5) the quadruped COM location should be between 148 mm to 298 mm away from the rear hip axes.

In addition to the above hard design constraints, the design should also follow the below design principles: (1) the robot should be as light as possible; (2) each leg should be designed as a relatively independent module so that the chassis could be easily changed and modified to fit different tail actuation modules; and (3) the quadruped COM should be at the center of its foothold polygon at the moment of jumping and the robot should have the design flexibility to adjust its COM location when a tail is mounted onto the quadruped.

III. DESIGN REALIZATION

Following the design requirements and design principles, this section presents the actual design choices for the robot.

A. Mechanical Design

The mechanical structure of the RCQ is presented in Fig. 6, where the robot consists of five relatively independent subassemblies: the front right (FR) leg,

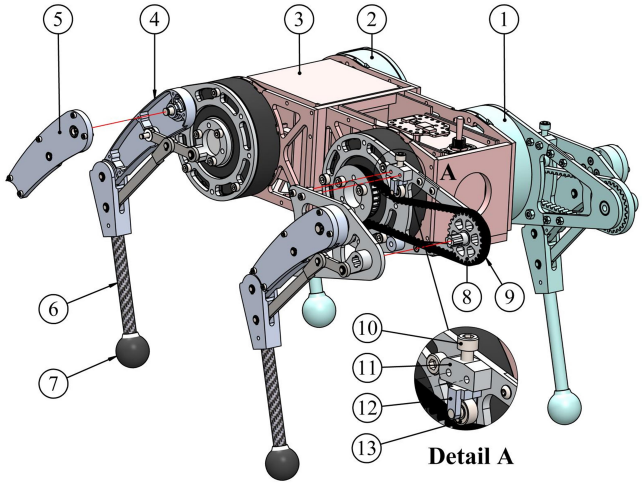

1: RR Leg
2: FR Leg
3: Chassis
4: Femur
5: Femur Cover
6: Tibia Tube
7: Foot
8: Timing Pulley
9: HTD Timing Belt
10: Tension Adjustment Screw
11: Tensioner Holder
12: Tensioner Slide Guide
13: Tensioner Wheel

Fig. 6: Mechanical structure of the RCQ: the FL and RL legs are in exploded views and the FR leg, RR leg, and the chassis are highlighted to show their modularity.

front left (FL) leg, rear right (RR) leg, rear left (RL) leg, and the chassis.

1) Actuator: Following the requirements sized in section II-B, the actuator hardware is chosen to be an improved version of the open-source MIT mini cheetah actuator [32], which has a fully enclosed (ip54 level) housing design with an overall weight of 610 g and a reduction ratio of 6. The actuator uses a brushless direct current (BLDC) electric motor inside, which is equivalent to the T-Motor U8. For such a configuration, each actuator is able to generate a peak torque of 17 Nm and a maximum speed of 40 rad/s at 24 V (peak current is around 30 A), which gives a total power of up to 680 W.

2) Leg Design: The legs are designed to be as light as possible so that their dynamic effects on the body could be minimized. To increase its strength and rigidity, the femurs and tibias are designed to have spatial structures. Carbon fiber tubes are utilized for the tibias to reduce weight and rubber feet are used to reduce the landing shock. Note that the small gearbox ratio of the actuator (quasi direct drive) allows designing a passive (without relying on sensor input) virtual spring-damper system on the foot by adjusting the controller parameters. The virtual spring stiffness on the foot is related to the stiffness on the crank (K_a, specified by the controller) by the foot Jacobians. Since the foot Jacobian has two components, there are two virtual springs on the foot too:

$$K_{f,*} = \frac{f_{f,*}}{\delta p_{f,*}} = \frac{\tau_c / j_{f,*}}{\delta \theta_1 j_{f,*}} = \frac{K_a}{j_{f,*}^2} \tag{5}$$

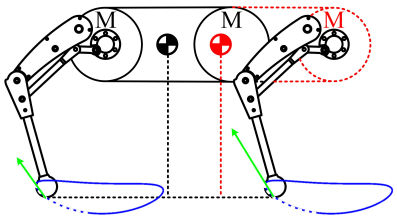

Fig. 7: Motor positions are important for relocating the RCQ COM location and thus improving its dynamic performance. The red lines indicate the robot configuration before motor relocation.

where $K_{f,*}$ is the virtual spring stiffness on the vertical (when * is n) or the horizontal direction (when * is h). The $\delta p_{f,*}$ and $\delta \theta_1$ are the small displacements of the foot and the crank, respectively. These two virtual springs could be also combined into one virtual spring K_f along the tangent direction of the foot trajectory:

$$K_f = \frac{f_f}{\delta p_f} = \frac{\tau_c MA}{\delta \theta_1 / MA} = K_a MA^2 \tag{6}$$

where f_f and δp_f are the force and small displacement on the foot along the tangent direction of its trajectory. $MA = 1/\sqrt{j_{f,n}^2 + j_{f,h}^2}$ is the mechanical advantage of the leg mechanism. Note that the f_f is not the resultant force of $f_{f,n}$ and $f_{f,h}$. From the above formulation, the virtual spring stiffness on the foot is related to the actuator stiffness by a square of the mechanical advantage. Properly selecting the K_a value before landing helps to eliminate a physical spring design on the foot.

3) Motor Relocation: Since the motors constitute most of the robot mass, their locations have a significant influence on the system COM location. Unlike other quadruped robots which usually have symmetric or identical actuator locations, the motor location of the RCQ leg mechanism is naturally behind its stance foothold locations. For instance, in Fig. 7, if the actuators were deployed to their natural positions, the system COM is naturally closer to the rear footholds. This causes a serious problem that the GRF might be always below the COM position at the moment of jumping and thus generates a positive moment, which in turn causes a head-up tip over motion. In fact, this COM location (150 mm) is just on the boundary of the required range, which is risky for design choices. To avoid this problem and to meet the design requirement, the actuator locations of the rear legs are shifted 136 mm ahead so that the system COM locates roughly above the midpoint of two representative footholds, which are the front and rear foothold locations just at the moment of jumping. This corresponds to a crank angle of -40 degrees. The actual COM location for the prototype measured in Solidworks is 207 mm, which is in the safe range of the requirement.

It is worth noting that the GRF (also appeared in Fig. 3b) generated by the foot is not exactly in the opposite direction of the foot motion which is along

the tangent line of the foot trajectory. In reality, the GRF is also affected by the motions of other legs. This makes it difficult to estimate the GRF direction and thus to determine the COM location through theoretical computation.

4) Powertrain: Because of the motor relocation for the rear legs, power transmission systems have to be used. Considering the transmitted torque and reliability, High Torque Drive (HTD) timing belts with a 5 mm pitch, a 6 mm width, and 82 teeth, are used. Corresponding belt tensioners (see detail A in Fig. 6) are also designed to adjust the belt tension. All the timing belt pulleys have the same tooth number (27 teeth) so that there is no additional reduction ratio on the powertrain system.

5) Chassis/Spine Bay: The main function of the chassis is to house the actuation module (spine) of the tail system. Therefore, it is designed to be an independent module from the legs. Their only connections are through the backside of the actuator. This design feature guarantees the design flexibility to fit the spine and adjust the overall COM when different tails were integrated into the quadruped.

B. Electrical Design

The schematic diagram of the RCQ electrical system is shown in Fig. 8, which mainly consists of two signal flows: a 24 V power supply signal flowing from a 7S1P LiPo battery (5 Ah capacity, 125 A continuous discharge rate, and 175 A burst discharge rate) into a power distribution board (PDB) to drive the four actuators, and a 3.3 V Controller Area Network (CAN) bus signal flowing between the microcontroller unit (MCU) and the motor drivers to send and receive control commands. The PDB also provides a 5 V power supply for the MCU and measures the current drawn from the battery. For the current design, the MCU is only responsible for simple control, collecting sensor data, and packaging CAN commands. The actual computation and higher-level control happen on the host computer. For future upgrades, a single board computer may be used so that all the real-time control and command packaging could happen on the robot.

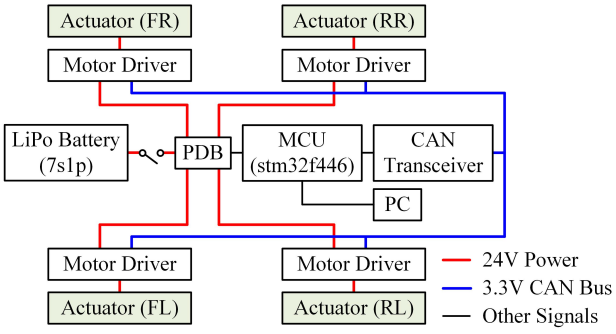

Fig. 8: Electrical system diagram

C. Low Level Control Structure

The controller architecture is similar to most mechatronic systems and consists of two control layers: a motion control layer to coordinate the motion of different joints and a joint control layer to track the individual joint trajectory. In the RCQ hardware, the joint control happens in the motor driver and is programmed to accept the torque command directly and/or the position command through a PD controller. Unlike other quadruped robots, one unique feature of the RCQ leg mechanism is that its crank requires a continuous rotation (instead of the back-and-forth motion for most quadruped robot actuators). This special feature requires the actuator to accept only incremental position commands, due to the limited size (0 - 64 bits) of the standard CAN frame. The CAN transceiver runs at a baud rate of 1 Mbps and each control loop consists of sending one command frame (around 120 bits) and receiving one sensor frame (around 100 bits). Therefore, after adding spaces between frames, to control four actuators using one bus, the maximum control frequency is $1M/250/4 = 1k$ Hz.

IV. EXPERIMENTS

The robot prototype is shown in Fig. 1. All the customized metal parts were made out of 6061-T6 aluminum alloy by a desktop Computer Numerical Control (CNC) milling machine with an accuracy of 0.01 mm. All the customized plastic parts were made out of Acrylonitrile Butadiene Styrene (ABS) using a 3D printer. The prototype weighs 5 Kg and has an overall height of 240 mm, an overall length of 440 mm, and an overall width of 220 mm. The following sections verify that the built robot meets the design requirements through experiments and simulations.

A. Jumping Ability

Since the robot is mainly developed for performing maneuvering (which requires the quadruped to be able to jump) and stabilization (which requires the quadruped to be able to walk) tasks after the tail is integrated, jumping ability is a critical metric to evaluate the design effectiveness, due to its higher requirement on the hardware's extreme performance. To conduct the jumping experiments, a high-speed camera (120 frames per second) and cardboard with a known grid size ($50mm \times 50mm$) were used. The robot crank angles were all set to -40 degrees, and a point-to-point position command of 2π with a proportional gain of 10 and a derivative gain of 1 was sent to each actuator simultaneously. Fig. 9 shows six snapshots of this jumping motion. Based on the camera recording, the jumping height was determined to be around 112 mm, which is 46.7% of its body height. The robot can stay in the air for at least 0.3 seconds. It is concluded that the jumping height is slightly under the design requirement.

To evaluate the jumping behavior, further comparisons to a simulation were also conducted. The simulation used

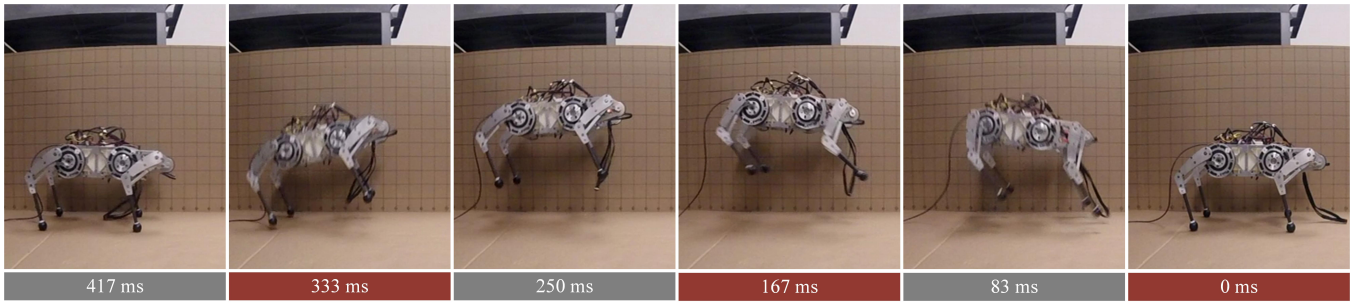

Fig. 9: Snapshots of the RCQ jumping motion (background wall is a $50mm \times 50mm$ grid cardboard)

the same simulation environment as in section II with the exception of adapting all the parameters (without tail) based on the real robot. Fig. 10 presents the two COM trajectories from the simulation and the experiment, where the $p_{p,y}$ and $p_{p,z}$ are the y and z component of the point P position, respectively (referring to Fig. 3a). The experimental data were obtained by manually counting the pixels of each frame. Therefore, the accuracy of the experimental data is estimated to be 5 mm. From the comparison, it can be found that the robot hardware tends to jump upward instead of forward. However, this tendency is preferred since, for the maneuvering task, the quadruped remaining longer in the air provides more time for the tail to swing in order to reorient the robot mid-air.

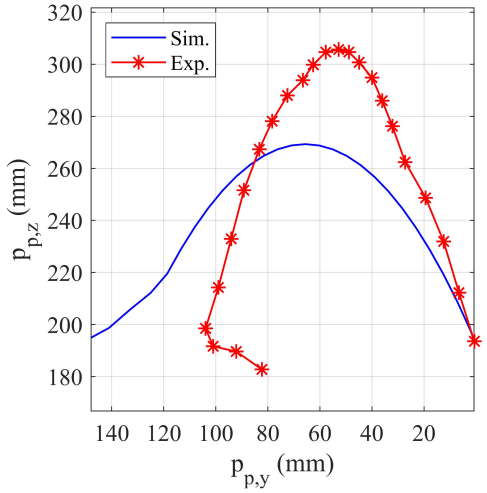

Fig. 10: Comparison of the COM trajectories for the experiment and the simulation

B. Tail Integration Ability

To show that the chassis/spine bay has the required room to fit the tail system, a tentative tail integration design was made. This design follows the design requirements from the simulation results in section II. The spine weight and dimensions were estimated based on the existing hardware of the R3RT [27] even though a smaller version may be used in reality. This gives a total weight of 1.95 Kg (three 100 W Maxon EC-i 40 motors plus gearheads) and an overall diameter of 90 mm for the spine assembly. Fig. 11 illustrates the tentative design where the red components constitute the actuation unit (spine) of the tail. It is shown that the system COM after integrating the tail is also located close to the foothold polygon center. It is worth noting that the original mass requirement for the spine is less than 1 Kg. The extra 0.95 Kg is from the saved 1 Kg weight from the quadruped (which ended up being 5 Kg instead of 6 Kg).

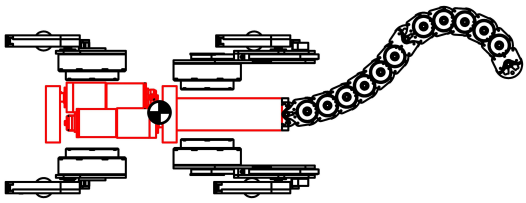

Fig. 11: One design example to integrate a typical serpentine robotic tail on the RCQ

V. CONCLUSIONS

In this paper, a quadruped robot platform that was designed for serpentine robotic tail research was developed. A systematical approach based on dynamic analysis was used to determine the critical design requirements and principles. Following the design requirements, a detailed design was carried out and a complete, functional prototype was built. Jumping experiments and corresponding simulations were conducted to verify the design requirements and to evaluate its performance. The results showed that the quadruped robot is able to jump to 46.7% of its body height and stay in the air for at least 0.3 seconds, which is sufficient for the maneuvering task when a robotic tail is integrated on the platform.

Our ongoing work includes integrating a serpentine robotic tail on the quadruped robot and developing a motion controller for the maneuvering task (airborne righting), which may require an upgrade to the electronics as well as some modifications to the spine bay design. Various gaits (e.g., bounding and trotting) will be also explored for the integrated robot. Since the long-term goal of this project is to explore the tail functions on general legged robots, integration and control of a

serpentine robotic tail on a general quadruped robot platform (e.g., the Mini Cheetah robot [32] or the Solo quadruped robot [33]) will be also an important future work.

References

[1] G. J. Zeglin, "Uniroo — a one legged dynamic hopping robot," Massachusetts Institute of Technology, Boston, MA, technical report, 1999.

[2] T. Libby, T. Y. Moore, E. Chang-Siu, D. Li, D. J. Cohen, A. Jusufi, and R. J. Full, "Tail-assisted pitch control in lizards, robots and dinosaurs," Nature, vol. 481, no. 7380, pp. 181–184, 2012.

[3] R. Briggs, J. Lee, M. Haberland, and S. Kim, "Tails in biomimetic design: Analysis, simulation, and experiment," in 2012 IEEE/RSJ International Conference on Intelligent Robots and Systems. IEEE, 2012, pp. 1473–1480.

[4] N. J. Kohut, A. O. Pullin, D. W. Haldane, D. Zarrouk, and R. S. Fearing, "Precise dynamic turning of a 10 cm legged robot on a low friction surface using a tail," in 2013 IEEE International Conference on Robotics and Automation. IEEE, 2013, pp. 3299–3306.

[5] E. Chang-Siu, T. Libby, M. Brown, R. J. Full, and M. Tomizuka, "A nonlinear feedback controller for aerial self-righting by a tailed robot," in 2013 IEEE International Conference on Robotics and Automation. IEEE, 2013, pp. 32–39.

[6] G.-H. Liu, H.-Y. Lin, H.-Y. Lin, S.-T. Chen, and P.-C. Lin, "A bio-inspired hopping kangaroo robot with an active tail," Journal of Bionic Engineering, vol. 11, no. 4, pp. 541–555, 2014.

[7] A. De and D. E. Koditschek, "Parallel composition of templates for tail-energized planar hopping," in 2015 IEEE International Conference on Robotics and Automation (ICRA). IEEE, 2015, pp. 4562–4569.

[8] A. Patel and E. Boje, "On the conical motion of a two-degree-of-freedom tail inspired by the cheetah," IEEE Transactions on Robotics, vol. 31, no. 6, pp. 1555–1560, 2015.

[9] J. Zhao, T. Zhao, N. Xi, M. W. Mutka, and L. Xiao, "Msu tailbot: Controlling aerial maneuver of a miniature-tailed jumping robot," IEEE/ASME Transactions on Mechatronics, vol. 20, no. 6, pp. 2903–2914, 2015.

[10] T. Libby, A. M. Johnson, E. Chang-Siu, R. J. Full, and D. E. Koditschek, "Comparative design, scaling, and control of appendages for inertial reorientation," IEEE Transactions on Robotics, vol. 32, no. 6, pp. 1380–1398, 2016.

[11] J. L. C. Santiago, I. S. Godage, P. Gonthina, and I. D. Walker, "Soft robots and kangaroo tails: modulating compliance in continuum structures through mechanical layer jamming," Soft Robotics, vol. 3, no. 2, pp. 54–63, 2016.

[12] S. W. Heim, M. Ajallooeian, P. Eckert, M. Vespignani, and A. J. Ijspeert, "On designing an active tail for legged robots: simplifying control via decoupling of control objectives," Industrial Robot: An International Journal, 2016.

[13] C. S. Casarez and R. S. Fearing, "Steering of an underactuated legged robot through terrain contact with an active tail," in 2018 IEEE/RSJ International Conference on Intelligent Robots and Systems (IROS). IEEE, 2018, pp. 2739–2746.

[14] B. Simon, R. Sato, J.-Y. Choley, and A. Ming, "Development of a bio-inspired flexible tail systemxs," in 2018 12th France-Japan and 10th Europe-Asia Congress on Mechatronics. IEEE, 2018, pp. 230–235.

[15] J. Norby, J. Y. Li, C. Selby, A. Patel, and A. M. Johnson, "Enabling dynamic behaviors with aerodynamic drag in lightweight tails," IEEE Transactions on Robotics, 2021.

[16] T. Fukushima, R. Siddall, F. Schwab, S. Toussaint, G. Byrnes, J. A. Nyakatura, and A. Jusufi, "Inertial tail effects during righting of squirrels in unexpected falls: From behavior to robotics," Integrative and Comparative Biology, 2021.

[17] W. S. Rone, W. Saab, A. Kumar, and P. Ben-Tzvi, "Controller design, analysis, and experimental validation of a robotic serpentine tail to maneuver and stabilize a quadrupedal robot," Journal of Dynamic Systems, Measurement, and Control, vol. 141, no. 8, 2019.

[18] D. Soto, K. Diaz, and D. I. Goldman, "Enhancing legged robot navigation of rough terrain via tail tapping," in Climbing and Walking Robots Conference. Springer, 2021, pp. 213–225.

[19] W. Saab, W. S. Rone, and P. Ben-Tzvi, "Robotic tails: a state-of-the-art review," Robotica, vol. 36, no. 9, pp. 1263–1277, 2018.

[20] BBC Earth. (2019, Oct.) Cheetahs are incredible predators! [Online]. Available: https://www.youtube.com/watch?v=UJMJryKXjkg (Retrieved 09/06/2021)

[21] Ninja Rat. (2019, Mar.) Kangaroo rat mid-air maneuver via tail rotation. [Online]. Available: https://www.youtube.com/watch?v=aV8_iv6SXqc (Retrieved 09/06/2021)

[22] M. Raibert, K. Blankespoor, G. Nelson, and R. Playter, "Bigdog, the rough-terrain quadruped robot," IFAC Proceedings Volumes, vol. 41, no. 2, pp. 10 822–10 825, 2008.

[23] C. Semini, N. G. Tsagarakis, E. Guglielmino, M. Focchi, F. Cannella, and D. G. Caldwell, "Design of hyq–a hydraulically and electrically actuated quadruped robot," Proceedings of the Institution of Mechanical Engineers, Part I: Journal of Systems and Control Engineering, vol. 225, no. 6, pp. 831–849, 2011.

[24] M. Hutter, C. Gehring, D. Jud, A. Lauber, C. D. Bellicoso, V. Tsounis, J. Hwangbo, K. Bodie, P. Fankhauser, M. Bloesch, et al., "Anymal-a highly mobile and dynamic quadrupedal robot," in 2016 IEEE/RSJ international conference on intelligent robots and systems (IROS). IEEE, 2016, pp. 38–44.

[25] S. Seok, A. Wang, M. Y. Chuah, D. J. Hyun, J. Lee, D. M. Otten, J. H. Lang, and S. Kim, "Design principles for energy-efficient legged locomotion and implementation on the mit cheetah robot," Ieee/asme transactions on mechatronics, vol. 20, no. 3, pp. 1117–1129, 2014.

[26] B. McInroe, H. C. Astley, C. Gong, S. M. Kawano, P. E. Schiebel, J. M. Rieser, H. Choset, R. W. Blob, and D. I. Goldman, "Tail use improves performance on soft substrates in models of early vertebrate land locomotors," Science, vol. 353, no. 6295, pp. 154–158, 2016.

[27] W. Saab, W. S. Rone, A. Kumar, and P. Ben-Tzvi, "Design and integration of a novel spatial articulated robotic tail," IEEE/ASME Transactions on Mechatronics, vol. 24, no. 2, pp. 434–446, 2019.

[28] S. Nansai, N. Rojas, M. R. Elara, R. Sosa, and M. Iwase, "On a jansen leg with multiple gait patterns for reconfigurable walking platforms," Advances in Mechanical Engineering, vol. 7, no. 3, p. 1687814015573824, 2015.

[29] Y. Liu and P. Ben-Tzvi, "An articulated closed kinematic chain planar robotic leg for high-speed locomotion," Journal of Mechanisms and Robotics, vol. 12, no. 4, 2020.

[30] M. Azad and R. Featherstone, "A new nonlinear model of contact normal force," IEEE Transactions on Robotics, vol. 30, no. 3, pp. 736–739, 2013.

[31] Y. Liu and P. Ben-Tzvi, "Dynamic modeling, analysis, and design synthesis of a reduced complexity quadruped with a serpentine robotic tail," Integrative and Comparative Biology, 2021.

[32] B. Katz, J. Di Carlo, and S. Kim, "Mini cheetah: A platform for pushing the limits of dynamic quadruped control," in 2019 international conference on robotics and automation (ICRA). IEEE, 2019, pp. 6295–6301.

[33] F. Grimminger, A. Meduri, M. Khadiv, J. Viereck, M. Wüthrich, M. Naveau, V. Berenz, S. Heim, F. Widmaier, T. Flayols, et al., "An open torque-controlled modular robot architecture for legged locomotion research," IEEE Robotics and Automation Letters, vol. 5, no. 2, pp. 3650–3657, 2020.